

Comparison of Boltzmann Equations with Quantum Dynamics for Scalar Fields

Manfred Lindner^{(a)*} and Markus Michael Müller^{(a,b)†}

*(a) Physik-Department T30d, Technische Universität München
James-Franck-Straße, 85748 Garching, Germany*

*(b) Max-Planck-Institut für Physik (Werner-Heisenberg-Institut)
Föhringer Ring 6, 80805 München, Germany*

Abstract

Boltzmann equations are often used to study the thermal evolution of particle reaction networks. Prominent examples are the computation of the baryon asymmetry of the universe and the evolution of the quark-gluon plasma after relativistic heavy ion collisions. However, Boltzmann equations are only a classical approximation of the quantum thermalization process which is described by the so-called Kadanoff-Baym equations. This raises the question how reliable Boltzmann equations are as approximations to the full Kadanoff-Baym equations. Therefore, we present in this paper a detailed comparison between the Kadanoff-Baym and Boltzmann equations in the framework of a scalar Φ^4 quantum field theory in 3+1 space-time dimensions. The obtained numerical solutions reveal significant discrepancies in the results predicted by both types of equations. Most notably, apart from quantitative discrepancies, on a qualitative level the universality observed for the Kadanoff-Baym equations is severely restricted in the case of Boltzmann equations.

*email: lindner@ph.tum.de

†email: Markus_Michael_Mueller@ph.tum.de

1 Introduction

One of the most attractive frameworks to explain the matter-antimatter asymmetry of the universe is the so-called leptogenesis mechanism [1–3]. Here, lepton number violating interactions in the early universe produce a lepton asymmetry which is subsequently converted to the observed baryon asymmetry by so-called sphaleron processes. For the dynamical generation of the lepton asymmetry it is necessary, that the universe was in a state out of thermal equilibrium [4]. The standard means to deal with this nonequilibrium situation are Boltzmann equations. However, it is well known that (classical) Boltzmann equations suffer from several shortcomings as compared to their quantum mechanical generalizations, the so-called Kadanoff-Baym equations. This motivates a comparison of Boltzmann and Kadanoff-Baym equations in order to assess the reliability of quantitative predictions of leptogenesis scenarios.

In addition to leptogenesis, there are various other systems which warrant a comparison between Boltzmann and Kadanoff-Baym equations: In particular, a strong motivation is furnished by relativistic heavy ion collision experiments which aim at testing the quark gluon plasma. In these experiments the quark gluon plasma is produced in a state far from equilibrium. Recently, however, experiments claimed that the approach to thermal equilibrium should happen very fast, and that the evolution of the quark gluon plasma could even be described by hydrodynamic equations [5–8], which arise as approximations to Boltzmann equations. In this context it is important to note that different quantities effectively thermalize on different time scales [9]. Thus, one might face the situation that although the full approach to thermal equilibrium takes a very long time, certain quantities, which are sufficient to describe the evolution of the quark gluon plasma, approach equilibrium values on much shorter time scales.

In order to derive Boltzmann equations from Kadanoff-Baym equations, one has to employ several approximations, among them a first-order gradient expansion and a quasi-particle (or on-shell) approximation [10–12]. However, it is known, that the gradient expansion cannot be justified for early times. Consequently, one might expect that Boltzmann equations fail to describe the early-time evolution and that errors accumulated for early times cannot be remedied at late times. Furthermore, as a consequence of the quasi-particle approximation, the conservation of momentum and energy prevents Boltzmann equations from describing thermalization in $1 + 1$ space-time dimensions. In contrast to this, it has been shown in the framework of a scalar Φ^4 quantum field theory that this is feasible with Kadanoff-Baym equations [13]. The reason for this qualitative discrepancy is that Kadanoff-Baym equations take off-shell effects into account [14], which are neglected in Boltzmann equations. Of course, in $3+1$ dimensions both types of equations are capable of describing thermalization. However, in the case of leptogenesis the on-shell character of the Boltzmann equation leads to a further inconsistency: All leptogenesis scenarios share the fact that some heavy particles decay out of thermal equilibrium into the particles which we observe in the universe today. The spectral function of a particle that can decay into other particles is given by a Breit-Wigner curve with a non-vanishing width. By employing the quasi-particle approximation we reduce this decay width of the particles to zero,

ie. a Boltzmann equation can only describe systems consisting of stable, or at least very long-lived, particles. After all, how does the on-shell character of the Boltzmann equation affect the description of quantum fields out of thermal equilibrium in $3 + 1$ dimensions?

When employing Boltzmann equations to the description of leptogenesis, the standard technique to construct the collision integrals — before employing further approximations — is to take the usual bosonic and fermionic statistical gain and loss terms multiplied with the S-matrix element for the respective reaction [15, 16]. These S-matrix elements are computed in vacuum, and one may wonder of which significance they are for a statistical quantum mechanical system.

All these shortcomings of Boltzmann equations lead to the conclusion that one should perform a detailed comparison between Boltzmann and Kadanoff-Baym equations [11, 17–19], such that one can explicitly see how large the quantum mechanical corrections are. Due to the complexity of the problem, we restrict ourselves for the moment to a Φ^4 quantum field theory in $3 + 1$ space-time dimensions. Of course, in this framework one can neither describe the phenomenon of leptogenesis nor thermalization after a heavy ion collision. Nevertheless, it permits to present a detailed comparison between Boltzmann and Kadanoff-Baym equations, which may point to interesting phenomena to be investigated in more realistic theories. Of course, it may also serve as a starting point for further research.

In general, when studying systems out of thermal equilibrium by means of Kadanoff-Baym equations, it is crucial to start from a Φ -derivable approximation, since these approximations ensure the conservation of energy and global charges [20–22]. The 2PI effective action furnishes such a Φ -derivable approximation [23–25]. In this work, we start from the 2PI effective action truncated at three-loop order. The Kadanoff-Baym equations can be obtained by requiring that the 2PI effective action be stationary with respect to variations of the full connected two-point function [13, 14]. In order to derive the corresponding Boltzmann equation, subsequently one has to employ a gradient expansion, a Wigner transformation, the Kadanoff-Baym ansatz and the quasi-particle approximation [10–12, 26, 27]. While the Boltzmann equation describes the time evolution of the particle number density, the Kadanoff-Baym equations describe the evolution of the full quantum mechanical two-point function of the system. However, one can define an effective particle number density which is given by the full propagator and its time derivatives evaluated at equal times [28]. Finally, we solve the Boltzmann and the Kadanoff-Baym equations numerically for spatially homogeneous and isotropic systems in $3+1$ dimensions and compare their predictions on the evolution of these systems for various initial conditions.

2 2PI Effective Action

In this work we consider a real scalar quantum field, whose dynamics is determined by the Lagrangian density

$$\mathcal{L} = -\frac{1}{2}(\partial_\mu \Phi)(\partial^\mu \Phi) - \frac{1}{2}m_B^2 \Phi^2 - \frac{\lambda}{4!} \Phi^4 .$$

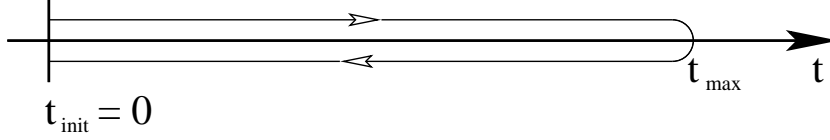


Figure 1: Closed real-time path \mathcal{C} . This time path was invented by Schwinger [29] (see also [30]) and applied to nonequilibrium problems by Keldysh [31]. In order to avoid the doubling of the degrees of freedom, we use the form presented in Ref. [11].

The minus sign of the kinetic term indicates that we use the metric where the time-time component is negative. As we will compute the evolution of the two-point Green's function for a nonequilibrium many body system, already the classical action has to be defined on the closed Schwinger-Keldysh real-time contour, shown in Fig. 1. The free inverse propagator can then be read off the free part of the classical action

$$I_0 = -\frac{1}{2} \int_c d^4x \int_c d^4y [\Phi(x) G_0^{-1}(x, y) \Phi(y)] ,$$

where

$$G_0^{-1}(x, y) = (\partial_{x^\mu} \partial_{y_\mu} + m_B^2) \delta_C(x - y) . \quad (1)$$

We consider a system without symmetry breaking, i.e. $\langle \Phi(x) \rangle = 0$. In this case the full connected Schwinger-Keldysh propagator is given by

$$G(x, y) = \langle T_C \{ \Phi(x) \Phi(y) \} \rangle .$$

Accordingly, for Gaussian initial conditions the 2PI effective action can be parameterized in the form [13, 23–25]

$$\Gamma[G] = \frac{i}{2} \text{tr}_C \log_C [G^{-1}] - \frac{1}{2} \text{tr}_C [G_0^{-1} G] + \Gamma_2[G] + \text{const} .$$

$i\Gamma_2[G]$ is the sum of all two-particle irreducible vacuum diagrams, where internal lines represent the full connected propagator $G(x, y)$. Of course, for an interacting theory we cannot compute $\Gamma_2[G]$ completely, and we have to rely on approximations. In this work we apply the loop expansion of the 2PI effective action up to three-loop order. The diagrams contributing to $\Gamma_2[G]$ in this approximation are shown in Fig. 2. We find [14]:

$$\begin{aligned} \Gamma_2[G] = & -\frac{\lambda}{8} \int_c d^4x [G(x, x) G(x, x)] \\ & + \frac{i\lambda^2}{48} \int_c d^4x \int_c d^4y [G(x, y) G(x, y) G(y, x) G(y, x)] . \end{aligned}$$

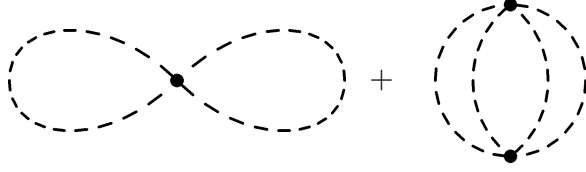


Figure 2: Two- and three-loop contribution to $\Gamma_2 [G]$. The lines represent the full connected Schwinger-Keldysh propagator.

3 Kadanoff-Baym Equations

The equation of motion for the full propagator reads [23, 24]

$$\frac{\delta\Gamma [G]}{\delta G (y, x)} = 0 .$$

It is equivalent to the Schwinger-Dyson equation

$$G^{-1} (x, y) = iG_0^{-1} (x, y) - \Pi (x, y) , \quad (2)$$

where the proper self energy is given by

$$\Pi (x, y) = 2i \frac{\delta\Gamma_2 [G]}{\delta G (y, x)} = -\frac{i\lambda}{2} \delta_C (x - y) G (x, x) - \frac{\lambda^2}{6} G (x, y) G (x, y) G (y, x) . \quad (3)$$

After we have inserted the free inverse propagator given in Eq. (1), we convolute the Schwinger-Dyson equation (2) with G from the right:

$$i \left(-\partial_{x^\mu} \partial_{x_\mu} + m_B^2 \right) G (x, y) = \delta_C (x - y) + \int_C d^4 z [\Pi (x, z) G (z, y)] \quad (4)$$

Next, we define the spectral function¹

$$G_\rho (x, y) = i \langle [\Phi (x), \Phi (y)]_- \rangle$$

and the statistical propagator²

$$G_F (x, y) = \frac{1}{2} \langle [\Phi (x), \Phi (y)]_+ \rangle$$

¹From the definition of the spectral function we see that it is antisymmetric in the sense that $G_\rho (x, y) = -G_\rho (y, x)$. Furthermore, the canonical equal-time commutation relations give $(G_\rho (x, y))_{x^0=y^0} = 0$ and $(\partial_{y^0} G_\rho (x, y))_{x^0=y^0} = -\delta^3 (\mathbf{x} - \mathbf{y})$.

²In contrast to the spectral function, the statistical propagator is symmetric in the sense that $G_F (x, y) = G_F (y, x)$.

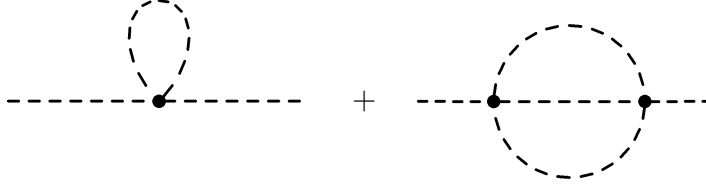


Figure 3: One- and two-loop contribution to the proper self-energy Π . Again, internal lines represent the full connected Schwinger-Keldysh propagator. The tadpole represents the local part which causes a mass shift only. The setting-sun diagram represents the nonlocal part and leads to thermalization.

such that we can write the full propagator as

$$G(x, y) = G_F(x, y) - \frac{i}{2} \text{sign}_{\mathcal{C}}(x^0 - y^0) G_{\varrho}(x, y) . \quad (5)$$

Note that for real scalar quantum fields both the statistical propagator and the spectral function are real-valued functions. The spectral function describes the particle spectrum of our theory. From its Wigner transform we can obtain the thermal mass and the decay width of the particles in our system. On the other hand we will define an effective particle number density given by the statistical propagator and its time derivatives evaluated at equal times. From Eq. (3) (and Fig. 3) we see that the self energy contains a local and a nonlocal part:

$$\Pi(x, y) = -i\delta_{\mathcal{C}}(x - y) \Pi^{(local)}(x) + \Pi^{(nonlocal)}(x, y) .$$

The local part of the self energy only causes a mass shift, which can be included in an effective mass:

$$M^2(x) = m_B^2 + \Pi^{(local)}(x) = m_B^2 + \frac{\lambda}{2} G_F(x, x) . \quad (6)$$

After inserting Eq. (5) into Eq. (3), we can decompose the nonlocal part of the self energy in exactly the same way as we did for the propagator:

$$\Pi^{(nonlocal)}(x, y) = \Pi_F(x, y) - \frac{i}{2} \text{sign}_{\mathcal{C}}(x^0 - y^0) \Pi_{\varrho}(x, y) .$$

We find

$$\Pi_F(x, y) = -\frac{\lambda^2}{6} \left(G_F(x, y) G_F(x, y) G_F(x, y) - \frac{3}{4} G_{\varrho}(x, y) G_{\varrho}(x, y) G_F(x, y) \right)$$

and

$$\Pi_{\varrho}(x, y) = -\frac{\lambda^2}{6} \left(3G_F(x, y) G_F(x, y) G_{\varrho}(x, y) - \frac{1}{4} G_{\varrho}(x, y) G_{\varrho}(x, y) G_{\varrho}(x, y) \right) .$$

When we insert all these definitions into Eq. (4), we observe that it splits into two complementary real-valued evolution equations for the statistical propagator and the spectral function, respectively [13]. These are the so-called Kadanoff-Baym equations:

$$(-\square_x + M^2(x)) G_F(x, y) = \int_0^{y^0} d^4z [\Pi_F(x, z) G_\rho(z, y)] - \int_0^{x^0} d^4z [\Pi_\rho(x, z) G_F(z, y)] \quad (7)$$

and

$$(-\square_x + M^2(x)) G_\rho(x, y) = - \int_{y^0}^{x^0} d^4z [\Pi_\rho(x, z) G_\rho(z, y)] . \quad (8)$$

For a spatially homogeneous system, one can Fourier transform these equations with respect to the spatial relative coordinate. Furthermore, in an isotropic system the propagator will depend only on the modulus of the momentum. As explained in more detail in Ref. [28], one can define effective kinetic energy and particle number densities $\omega(t, \mathbf{p})$ and $n(t, \mathbf{p})$ which are given by the statistical propagator and its derivatives, evaluated at equal times:

$$\omega^2(t, \mathbf{p}) = \left(\frac{\partial_{x^0} \partial_{y^0} G_F(x^0, y^0, \mathbf{p})}{G_F(x^0, y^0, \mathbf{p})} \right)_{x^0=y^0=t} \quad (9)$$

and

$$n(t, \mathbf{p}) = \omega(t, \mathbf{p}) G_F(t, t, \mathbf{p}) - \frac{1}{2} . \quad (10)$$

However, we stress that the Kadanoff-Baym equations are self-consistent evolution equations for the full propagator of our system, and that one has to follow the evolution of the two-point function throughout the whole x^0 - y^0 -plane (of course, constrained to the part with $x^0 \geq 0$ and $y^0 \geq 0$). One can then follow the evolution of the effective particle number density along the bisecting line of this plane.

We would like to emphasize that the only approximation involved in the numerical solution of the Kadanoff-Baym equations is the loop expansion of the 2PI effective action. In the next section we will describe the approximations which are necessary to derive a Boltzmann equation from the Kadanoff-Baym equation for the statistical propagator (7).

4 Boltzmann Equations

It is well known how Boltzmann equations can be obtained as an approximation of the Kadanoff-Baym equations [10–12]. In this section we briefly review the standard derivation: One has to employ a Wigner transformation, a gradient expansion, the Kadanoff-Baym ansatz and the quasi-particle approximation.

First, we subtract the Hermitian adjoint of Eq. (7) from Eq. (7) and re-parameterize the propagator and the self energy by center and relative coordinates

$$G(u, v) = \tilde{G}\left(\frac{u+v}{2}, u-v\right).$$

Next, we define $X = \frac{x+y}{2}$ and $s = x - y$, and observe on the left hand side of the difference equation that

$$\square_x - \square_y = 2\partial_{s\mu}\partial_{X\mu}$$

is automatically of first order in ∂_X . Furthermore, we Taylor expand the effective masses on the left hand side as well as the propagators and self energies on the right hand side to first order in ∂_X around X . After that, we Fourier transform the difference equation with respect to s . The Wigner transformed statistical propagator and spectral function are given by

$$\tilde{G}_F(X, k) = \int d^4s \exp(iks) \tilde{G}_F(X, s)$$

and

$$\tilde{G}_\rho(X, k) = -i \int d^4s \exp(iks) \tilde{G}_\rho(X, s),$$

respectively. The factor of $-i$ in the Wigner transform of the spectral function makes $\tilde{G}_\rho(X, k)$ again a real-valued function. However, in order to be able to really perform the Fourier transform, we have to send the initial time to $-\infty$. At least for large x^0 and y^0 this can be justified by taking into account that correlations between earlier and later times are suppressed exponentially, as one can see in Fig. 5. The result of all these transformations is a quantum kinetic equation for the statistical propagator³ [32–34]:

$$\begin{aligned} & (2k^\mu\partial_{X\mu} + (\partial_{X\mu}M^2(X))\partial_{k\mu})\tilde{G}_F(X, k) \\ &= \tilde{G}_F(X, k)\tilde{\Pi}_\rho(X, k) - \tilde{G}_\rho(X, k)\tilde{\Pi}_F(X, k) \\ &+ \left\{ \tilde{\Pi}_F(X, k); \text{Re}\left(\tilde{G}_R(X, k)\right) \right\}_{PB} + \left\{ \text{Re}\left(\tilde{\Pi}_R(X, k)\right); \tilde{G}_F(X, k) \right\}_{PB}, \end{aligned} \quad (11)$$

where the Poisson brackets are defined by

$$\left\{ \tilde{f}(X, k); \tilde{g}(X, k) \right\}_{PB} = \left[\partial_{k\mu}\tilde{f}(X, k) \right] \left[\partial_{X\mu}\tilde{g}(X, k) \right] - \left[\partial_{X\mu}\tilde{f}(X, k) \right] \left[\partial_{k\mu}\tilde{g}(X, k) \right]. \quad (12)$$

³The retarded propagator $G_R(x, y) = \theta(x^0 - y^0)G_\rho(x, y)$ and self energy, as well as the corresponding advanced quantities, have to be introduced in order to remove the upper boundaries of the memory integrals. As a result the complete system of quantum kinetic equations includes six equations: one equation for $G_F, G_\rho, G_R, \Pi_F, \Pi_\rho$ and Π_R , respectively.

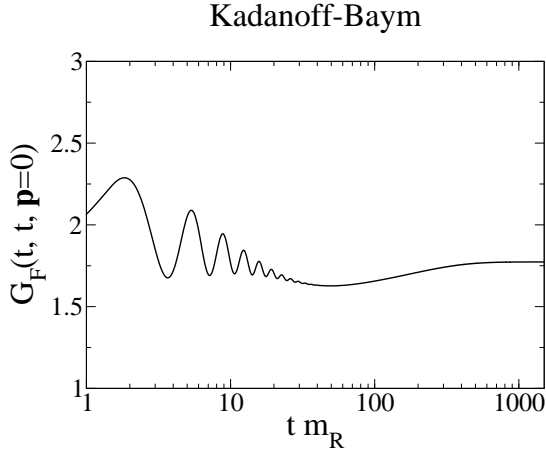


Figure 4: The equal-time propagator as a function of time for fixed momentum mode $\mathbf{p} = 0$. The system shows rapid oscillations which die out after moderate times and are followed by a smooth drifting regime.

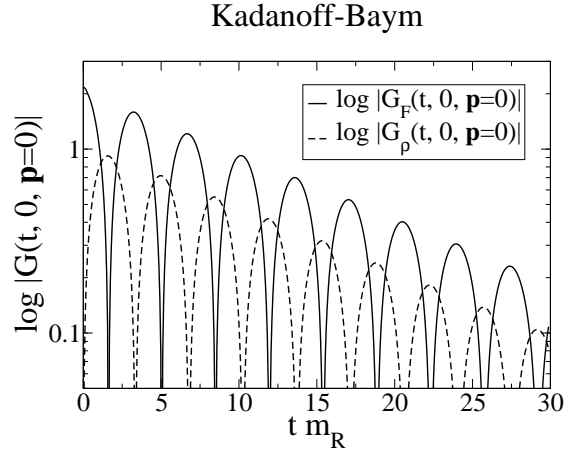


Figure 5: The modulus of the unequal-time propagator as function of time for fixed momentum mode $\mathbf{p} = 0$. Correlations between earlier and later times are exponentially damped.

Employing the first order Taylor expansion is clearly not justifiable for early times when the equal-time propagator is rapidly oscillating. But this is obvious, since employing this gradient expansion is clearly motivated by equilibrium considerations: In equilibrium the propagator depends on the relative coordinates only. There is no dependence on the center coordinates, and one may hope that there are situations where the propagator depends only moderately on the center coordinates. This is clearly the case for late times when our system is sufficiently close to equilibrium. However, as is shown in Fig. 4, already after moderate times the rapid oscillations mentioned above, have died out and are followed by a smooth drifting regime [13]. In this drifting regime the second derivative with respect to X should be negligible as compared to the first order derivative and a consistent Taylor expansion can be justified even though the system may still be far from equilibrium. However, it is crucial that the Taylor expansion is performed consistently for two reasons: First, this guarantees that the quantum kinetic equations satisfy exactly the same conservation laws as the full Kadanoff-Baym equations do [27]. Second, it has been shown that neglecting the Poisson brackets leads to equations whose range of validity is quite restricted [35]. For the intermediate and late-time regimes these quantum kinetic equations however have the advantage that they do not include any memory integrals. Being local in time, their numerical solution requires much less computer memory as for the case of the Kadanoff-Baym equations. Furthermore, the energy convolutions replacing the memory integrals can be done quite efficiently using a Fast Fourier Transform algorithm. In order to obtain a Boltzmann equation from the quantum kinetic equation (11), first we

have to discard the Poisson brackets. After that, we employ the Kadanoff-Baym ansatz

$$\tilde{G}_F(X, k) = \tilde{G}_\rho(X, k) \left(\tilde{n}(X, k) + \frac{1}{2} \right) \quad (13)$$

which also can be motivated by equilibrium considerations. This is a generalization of the fluctuation dissipation theorem, which states that, for a system in thermal equilibrium, the statistical propagator is proportional to the spectral function. The fluctuation dissipation theorem can be recovered from Eq. (13) by discarding the dependence on the center coordinate X and fixing \tilde{n} to be the Bose-Einstein distribution function. The last approximation, which is necessary to arrive at the Boltzmann equation, is the so-called quasi-particle (or on-shell) approximation:

$$\tilde{G}_\rho(X, k) = \frac{\pi}{E(X, \mathbf{k})} \left(\delta(k^0 - E(X, \mathbf{k})) - \delta(k^0 + E(X, \mathbf{k})) \right), \quad (14)$$

where the quasi-particle energy is given by

$$E(X, \mathbf{k}) = \sqrt{M^2(X) + \mathbf{k}^2}.$$

However, we would like to stress that the exact time evolution of the spectral function is determined by the Kadanoff-Baym equations. It has been shown that the spectral function can be parameterized by a Breit-Wigner function with a non-vanishing width [14, 19]. To reduce the width of this Breit-Wigner curve to zero is certainly not a controllable approximation and leads to very large qualitative discrepancies between the results produced by Kadanoff-Baym and Boltzmann equations. In fact this approximation can only be justified if our system consists of stable, or at least very long-lived, quasi-particles, whose mass is much larger than their decay width. We define the quasi-particle number density by

$$n(X, \mathbf{k}) = \tilde{n}(X, \mathbf{k}, E(X, \mathbf{k})).$$

After equating the positive energy components in Eq. (11) we arrive at the Boltzmann equation. For a spatially homogeneous system there is no dependence on the spatial center coordinates and the Boltzmann equation reads⁴:

$$\begin{aligned} \partial_t n(t, \mathbf{k}) = & \frac{\lambda^2 \pi}{48} \int \frac{d^3 p}{(2\pi)^3} \int \frac{d^3 q}{(2\pi)^3} \int d^3 r \left[\frac{1}{E_k E_p E_q E_r} \right. \\ & \times \delta(\mathbf{k} + \mathbf{p} - \mathbf{q} - \mathbf{r}) \delta(E_k + E_p - E_q - E_r) \\ & \left. \times \left((1 + n_{\mathbf{k}})(1 + n_{\mathbf{p}}) n_{\mathbf{q}} n_{\mathbf{r}} - n_{\mathbf{k}} n_{\mathbf{p}} (1 + n_{\mathbf{q}})(1 + n_{\mathbf{r}}) \right) \right]. \end{aligned} \quad (15)$$

For a spatially homogeneous system the effective mass also depends only on the time coordinate and, according to Eqs. (6), (13) and (14), is given by the following gap equation:

$$M^2(t) = m_B^2 + \frac{\lambda}{2} \int \frac{d^3 p}{(2\pi)^3} \left[\frac{2n(t, \mathbf{p}) + 1}{\sqrt{M^2(t) + \mathbf{p}^2}} \right]. \quad (16)$$

⁴Here, we use the abbreviations $E_k = \sqrt{M^2(t) + \mathbf{k}^2}$ and $n_{\mathbf{k}} = n(t, \mathbf{k})$.

For a spatially homogeneous and isotropic system we can go further and dramatically simplify the collision integral in the Boltzmann equation. The details of this calculation are shown in the appendix. The result is the following equation⁵:

$$\begin{aligned} \partial_t n(t, k) = & \frac{\lambda^2}{96\pi^4} \int_0^\infty dp \int_0^\infty dq \left[\Theta(r_0^2) \frac{pqD(k, p, q, r_0)}{E_k E_p E_q} \right. \\ & \left. \times \left((1 + n_k)(1 + n_p)n_q n_{r_0} - n_k n_p(1 + n_q)(1 + n_{r_0}) \right) \right]. \end{aligned} \quad (17)$$

The auxiliary functions r_0 and D are obtained from very simple expressions which are given in the appendix.

In this section we have shown that, using a gradient expansion and a quasi-particle (or on-shell) approximation, one can derive the Boltzmann equation from the Kadanoff-Baym equations. In this sense one can consider the Kadanoff-Baym equations as *quantum Boltzmann equations* re-summing the gradient expansion up to infinite order and including off-shell effects. In the next section we are going to explain how we solved the Boltzmann and the Kadanoff-Baym equations numerically.

5 Numerical Implementation

5.1 Kadanoff-Baym Equations

For the numerical simulations of the Kadanoff-Baym equations we follow exactly the lines of Refs. [13, 36, 37], ie. for the spatial coordinates we employ a standard discretization on a three-dimensional lattice with lattice spacing a_s and N_s lattice sites in each direction. Thus, the lattice momenta are given as usual by

$$\hat{p}_{n_j} = \frac{2}{a_s} \sin\left(\frac{\pi n_j}{N_s}\right),$$

where n_j , $j \in \{1, 2, 3\}$, enumerates the momentum modes in the j -th dimension. As we consider a spatially homogeneous and isotropic system, for given times (x^0, y^0) we only need to store the propagator for momentum modes with $\frac{N_s}{2} \geq n_1 \geq n_2 \geq n_3 \geq 0$. This saves us a factor of 48 in memory usage. The discretization in time leads to a history matrix $H = \{0, a_t, 2a_t, \dots, (N_t - 1)a_t\}^2$. Here a_t is the step size and N_t is the number of times in each time dimension for which we keep the propagator in memory in order to compute the memory integrals. This history cut off can be justified by the exponential damping of the unequal-time propagator, cf. Fig. 5. Exploiting the symmetry of the statistical propagator with respect to the interchange of its time arguments, we only need to store the values of the statistical propagator for $x^0 \geq y^0$. In very much the same way we can

⁵Now, $k = |\mathbf{k}|$ and $n_k = n(t, |\mathbf{k}|)$

use the respective antisymmetry of the spectral function. This saves us another factor of 2 in memory usage. The convolutions arising in the computation of the setting-sun self-energies are most efficiently computed using a Fast Fourier Transform algorithm for real-valued even functions [38].

In order to set the scale for the simulations, we use the renormalized vacuum mass m_R . The corresponding bare mass m_B is obtained through a perturbative renormalization at one-loop order of the self energy (tadpole) [39]. We solved the Kadanoff-Baym equations numerically on a lattice with $N_t = 500$, $N_s = 32$, $a_t m_R = 0.06$, $a_s m_R = 0.5$ and $\lambda = 18$. So far we performed our simulations on a simple desktop PC with a Pentium4 processor and 2 GByte RAM. However, we would like to note that the numerics can easily be parallelized.

5.2 Boltzmann Equation

In the discretized version of the Boltzmann equation (17) the momenta are of the form

$$p_n = \frac{\pi}{a_s N_s} n .$$

Using the same value for a_s as for the Kadanoff-Baym equations, also leads to the same momentum cutoff. Of course, N_s need not be the same as for the Kadanoff-Baym equations, which just means that we approach the infinite volume limit independently for both types of equations.

In order to compute the collision integral we proceed as follows: For fixed (k, p, q) we determine r_0 (the exact definition of r_0 is given in the appendix), which of course need not be one of the discretized momenta given above. The function $D(k, p, q, r_0)$ can be evaluated for any value of r_0 (as one also can see in the appendix). To obtain the particle number density for an arbitrary r_0 we use a cubic spline [40]. Thus, for given (k, p, q) the integrand is known to any given accuracy and for given k we can simply sum over p and q .

In order to advance in time we use a Runge-Kutta-Cash-Karp routine with adaptive step-size control [40]. At each time step we have to determine the effective mass from the gap equation (16). As it does not depend on the integration variable on the right hand side, we can find it by using a simple one dimensional root finding algorithm, namely a Steffenson method [40].

In order to set the scale for the simulations, again we use the renormalized vacuum mass m_R . Our simulations were done with $N_s = 500$, $a_s m_R = 0.5$ and $\lambda = 18$.

6 Comparing Boltzmann vs. Kadanoff-Baym

We consider three different initial conditions which correspond to the same average energy density. The corresponding initial particle number densities are shown in Fig. 6. These particle number densities can immediately be fed into the numerics for the Boltzmann equation. In order to obtain the initial conditions for the Kadanoff-Baym equations, we

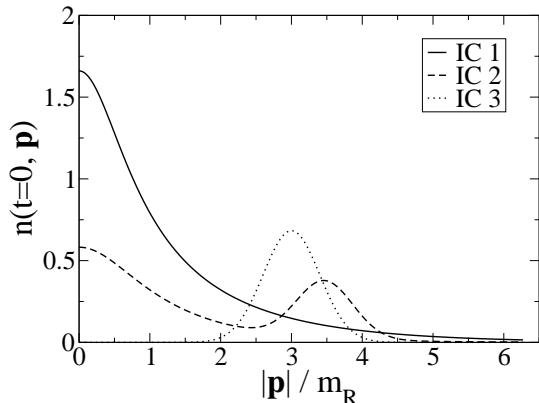


Figure 6: **Initial particle number densities** against absolute momenta. Shown are the three different initial conditions (IC) discussed in the text, for which we numerically solved the Boltzmann and the Kadanoff-Baym equations, respectively.

follow [28]: For a given initial particle number density, the initial values for the statistical propagator and its derivatives are determined according to:

$$G_F(x^0, y^0, \mathbf{p})_{x^0=y^0=0} = \left[\frac{n(t, \mathbf{p}) + \frac{1}{2}}{\omega(t, \mathbf{p})} \right]_{t=0}, \quad (18)$$

$$[\partial_{x^0} G_F(x^0, y^0, \mathbf{p})]_{x^0=y^0=0} = 0, \quad (19)$$

$$[\partial_{x^0} \partial_{y^0} G_F(x^0, y^0, \mathbf{p})]_{x^0=y^0=0} = \left[\omega(t, \mathbf{p}) \left(n(t, \mathbf{p}) + \frac{1}{2} \right) \right]_{t=0}, \quad (20)$$

where the initial effective energy density is given by

$$\omega(t=0, \mathbf{p}) = \sqrt{m_R^2 + \mathbf{p}^2}.$$

On the other hand, the initial values for the spectral function are determined from the canonical commutation relations.

Figs. 7 and 8 show the evolution of the particle number densities for two momentum modes ($|\mathbf{p}| = 0$ and $|\mathbf{p}| = 1.16m_R$) and the corresponding equilibrium particle number densities, respectively, for all initial conditions. In the left plots we can see, that the Kadanoff-Baym equations lead to a universal equilibrium particle number density. The left plot in Fig. 7 shows that the particle number densities show quite a different evolution for early times. However, respecting universality, for any given momentum mode they all approach the same late-time value. This plot is supplemented by the left plot in Fig. 8. There, one can see that the various particle number densities, after equilibrium has effectively been reached, indeed completely agree. Hence, this plot proves that we could have shown plots similar to the left one in Fig. 7 for all momentum modes. In particular the predicted temperature, given by the inverse slope of the line, is the same for all initial

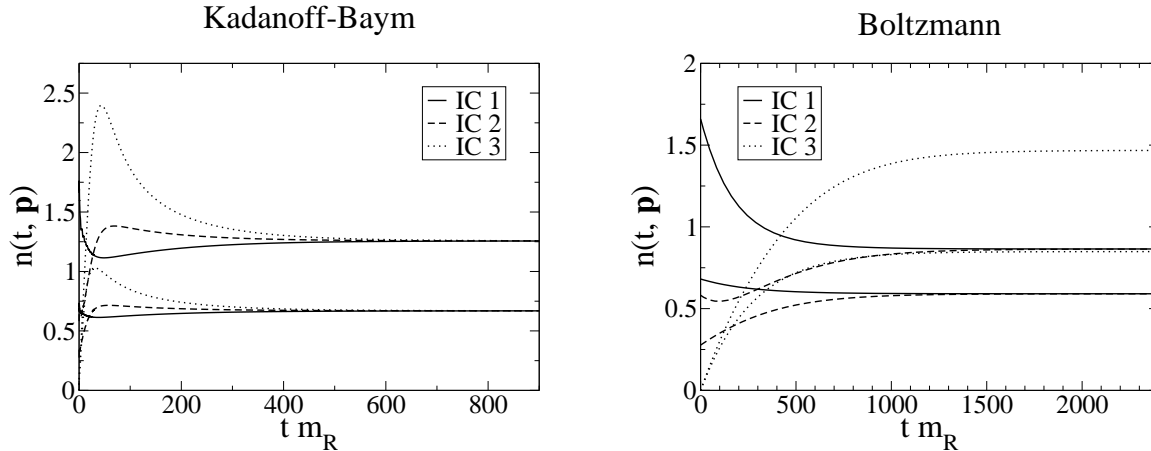


Figure 7: These plots show the **time evolution of the particle number densities** for two different momentum modes and all initial conditions (cf. Fig. 6) as determined by the Boltzmann and the Kadanoff-Baym equations, respectively. We see that the Kadanoff-Baym equations respect full universality, whereas in the case of the Boltzmann equation only a restricted universality is maintained, cf. Fig. 8.

conditions. However, the right plots reveal that the Boltzmann equation respects only a restricted universality. The right plot in Fig. 7 shows that, in general (e.g. for the initial conditions "IC 1" and "IC 3"), for any given momentum mode the particle number densities will not approach the same late-time value. For both momentum modes shown in the plot a considerable discrepancy is revealed. However, for the special case of the initial conditions "IC 1" and "IC 2" the late-time results do agree. Again, this plot is supplemented by the corresponding plot in Fig. 8: The lines for the initial conditions "IC 1" and "IC 2" completely agree, while the one for the initial condition "IC 3" deviates. One can see that there is only one momentum mode for which the late-time values of all particle number densities agree, namely the intersection point of the lines. However, we would like to stress, that we could easily have chosen a fourth initial condition for which the late-time result would intersect the lines in Fig. 8 in different points. Then there would be not a single momentum mode for which the late-time values of all particle number densities would agree.

The reason for the observed restriction of universality can be extracted from Fig. 9. There we show the time evolution of the total particle number per volume

$$N_{tot}(t) = \int \frac{d^3p}{(2\pi)^3} n(t, \mathbf{p}) .$$

In general the Kadanoff-Baym equations conserve the average energy density⁶ and global

⁶Concerning our simulations, of course, this only holds up to numerical errors. We have checked that our simulations conserve the average energy density up to a numerical uncertainty of 0.3% for the Kadanoff-Baym equations and 0.5% for the Boltzmann equation.

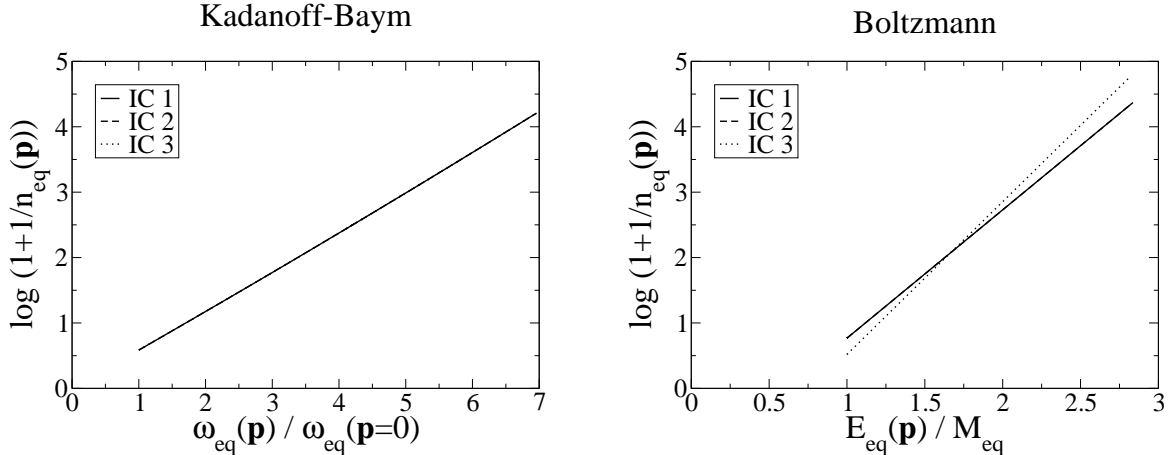


Figure 8: Here, we plotted the **equilibrium particle number densities** obtained for times when thermal equilibrium has effectively been reached, against the corresponding thermal energy densities. For a given initial condition, the inverse temperature β is given by the slope of the line and the chemical potential is obtained from the y-axis intercept divided by $-\beta$. Supplementing Fig. 7 we observe full (restricted) universality in the case of the Kadanoff-Baym (Boltzmann) equations.

charges [20–22]. However, as there is no conserved charge in our theory, the total particle number need not be conserved. Indeed, the Kadanoff-Baym equations include off-shell particle creation and annihilation [14]. As a result the total particle number may change, and in fact approaches a universal equilibrium value. However, in order to derive the Boltzmann equation from the Kadanoff-Baym equations, we had to employ the quasi-particle (or on-shell) approximation. As a result processes which would change the particle number are kinematically forbidden. The Boltzmann equation only includes two-particle scattering, which leaves the total particle number constant. Of course, this additional constant of motion severely restricts the evolution of the particle number density. Therefore the Boltzmann equation cannot lead to a universal quantum thermal equilibrium. Only initial conditions for which the average energy density and the total particle number agree from the very beginning, lead to the same equilibrium results.

In a system allowing for creation and annihilation of particles, the chemical potential of particles, whose total number is not restricted by any conserved quantity, must vanish in thermodynamical equilibrium. The chemical potential predicted by the Kadanoff-Baym and Boltzmann equations, respectively, is given by the y-axis intercept, extracted from Fig. 8, divided by $-\beta$. Using a ruler the reader might convince himself that the Kadanoff-Baym equations indeed lead to a universally vanishing chemical potential. In contrast to this, even without a ruler one can see that the Boltzmann equation, in general, will lead to a non-vanishing chemical potential⁷.

⁷For the initial conditions considered in this work, the Boltzmann equation predicted even a positive chemical potential. However, already on very general grounds, one can deduce that the chemical potential

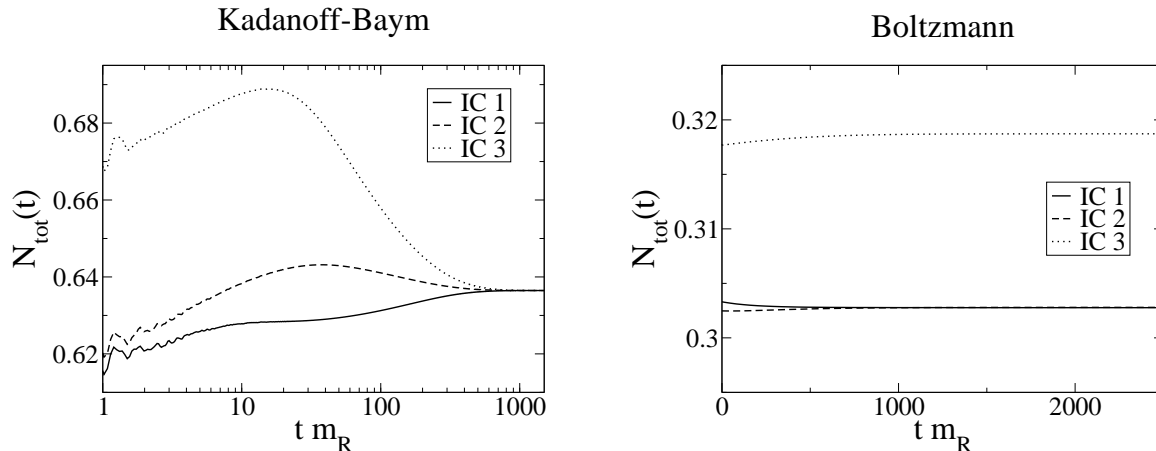


Figure 9: **Time evolution of the total particle number.** As expected from Ref. [14], the Kadanoff-Baym equations include off-shell particle creation and annihilation. As a result the total particle number may change with time. In contrast to this the total particle number is strictly conserved in the case of the Boltzmann equation. Concerning our simulations, of course, this only holds up to numerical errors ($< 0.4\%$).

In this context, Fig. 10 reveals some interesting results. In the upper left plot one can see that our tsunami initial condition is washed out quite rapidly. The full straight line in the lower left plot corresponds to the equilibrium particle number density. The double-dashed-dotted lines in both plots correspond to the particle number density at the same time $tm_R = 46.7$. Thus, in the lower left plot one obtains an approximate straight line already after a relatively short period of time, indicating a swift approach to kinetic equilibrium. Subsequently, this straight line is tilted until it intersects the origin of our coordinate system, corresponding to a vanishing chemical potential. However, this approach to full thermodynamical (including chemical) equilibrium takes a considerably longer time. In this way, the left plots reveal two distinct time scales: a rather fast kinetic equilibration, and a very slow thermodynamical (including chemical) equilibration. These two time scales can also be identified in the left plot of Fig. 7. The over-shooting of the particle number density for early times leads to the kinetic equilibration. In fact, the double-dashed-dotted line corresponds to the time, when the particle number density reaches its maximum value. The following rather long tail, again indicates that full thermalization takes place on much larger time scales. The corresponding plots on the right hand side show that it takes a much longer time for the Boltzmann equation to reach kinetic equilibrium. Furthermore, in contrast to the Kadanoff-Baym equations there is no explicit chemical equilibration indicating that the Boltzmann equation cannot distinguish between kinetic and thermodynamical equilibrium. As a result the Boltzmann equation may lead to a non-vanishing chemical potential. As already mentioned this chemical nonequilibrium originates from the conservation of the total particle number. In the case of the Kadanoff-Baym equations kinetic and chemical

for a boson gas has to be negative!

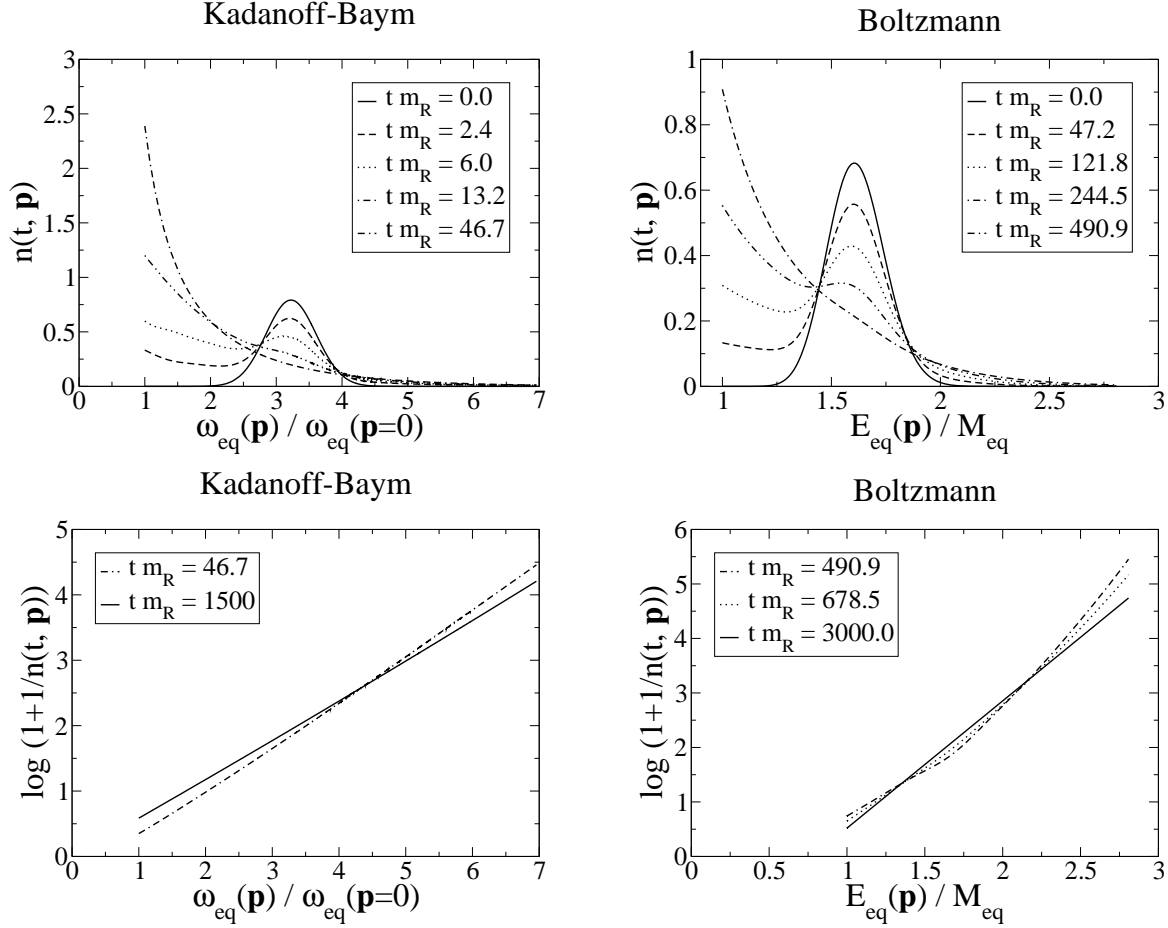


Figure 10: **Chemical (non)equilibration for "IC 3"**. The particle number density is shown against the equilibrium energy density at various times for initial condition "IC 3".

equilibration took place on different time scales. Due to the lack of chemical equilibration, there is no such separation of time scales in the case of the Boltzmann equation.

Eventually, Fig. 11 exhibits the evolution of the thermal masses. In the case of the Kadanoff-Baym equations, the thermal mass is given by the zero mode of the effective kinetic energy density (11). On the other hand, the thermal mass appearing in the Boltzmann equation is given by the effective mass (16). Again, for the Kadanoff-Baym equations full universality is respected and a common equilibrium value approached, while for the Boltzmann equation only the restricted universality is preserved. The corresponding late-time values are used to set the scale in Figs. 8 and 10. Concerning time scales, it is interesting to observe a similar behavior as discussed above. In the case of the Kadanoff-Baym equations, for early times we find rapid oscillations which are damped on approximately the same time scale as was observed for kinetic equilibration. Furthermore, the approach to the universal late-time value takes place on a time scale similar to the one observed

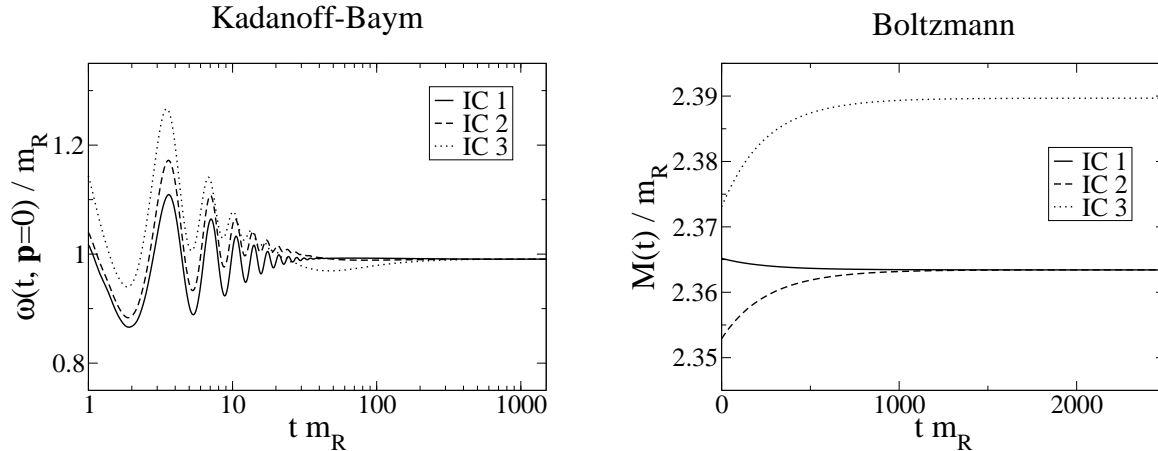


Figure 11: **Time Evolution of the thermal masses.** Again, for the Kadanoff-Baym (Boltzmann) equations we find full (restricted) universality. The late time values of the thermal (effective) masses are used to set the scale in Figs. 8 and 10.

for chemical equilibration. As already discussed above, there is no such separation of time scales in the case of the Boltzmann equation. As a matter of fact the effective masses hardly change their values. These values, however, should not be taken too seriously: Following the standard derivation as presented in Ref. [12], in the effective mass we omitted the real part of the nonlocal (setting-sun) self-energy. We would like to note, that an inclusion of this nonlocal contribution to the self energy would only change the values of the effective mass. Still, the total particle number would be conserved and the main result of this work would remain untouched: The full universality respected by the Kadanoff-Baym equations is severely restricted in the case of the Boltzmann equation.

7 Conclusions

Starting from the 2PI effective action for a scalar Φ^4 quantum field theory we briefly reviewed the derivation of the Kadanoff-Baym equations and the approximations which are necessary to eventually arrive at a Boltzmann equation. We solved both, the Kadanoff-Baym equations and the Boltzmann equation, numerically for spatially homogeneous and isotropic systems in 3+1 dimensions without any further approximations.

We have shown that the Kadanoff-Baym equations respect universality: For systems with equal average energy density the late time behavior coincides independent of the details of the initial conditions. In particular, independent of the initial conditions the particle number densities, temperatures and thermal masses predicted for times when equilibrium has effectively been reached coincide. The chemical potentials also coincide and vanish. Furthermore, we observed that thermalization takes place on two different time-scales: a rather fast kinetic equilibration, and a very slow thermodynamical (including chemical) equilibration.

In general the Kadanoff-Baym equations conserve the total energy as well as global charges. In the special case of a scalar Φ^4 quantum field theory the quasi-particle approximation implies that the Boltzmann equation also conserves the total particle number. This additional constant of motion severely restricts the evolution of the system. As a result the Boltzmann equation cannot lead to a universal quantum thermal equilibrium. The Boltzmann equation respects only a restricted universality: Only initial conditions for which the average energy density and the total particle number agree from the very beginning, lead to the same equilibrium results. In particular, the Boltzmann equation cannot describe the phenomenon of chemical equilibration and, in general, will lead to a non-vanishing chemical potential. Due to the lack of chemical equilibration, the separation of time scales, which we observed for the Kadanoff-Baym equations, is absent in the case of the Boltzmann equation.

Some of the approximations that lead from the Kadanoff-Baym equations to the Boltzmann equation (namely, the gradient expansion, neglecting the Poisson brackets and the Kadanoff-Baym ansatz) are clearly motivated by equilibrium considerations. Taking the observed restriction of universality into account, one can conclude that one can safely apply the Boltzmann equation only to systems which are sufficiently close to equilibrium. Accordingly, for a system far from equilibrium the results given by the Boltzmann equation should be treated with care.

One of the main motivations for this work was leptogenesis, where Boltzmann equations are the standard tool and where one frequently has to analyze the chemical potential. According to our results, these analyses should be treated with care, because, even in our rather simple model, the Boltzmann equation could not predict the chemical potential correctly.

Concerning the numerical implementation, however, the Boltzmann equation has some advantages as compared to the Kadanoff-Baym equations. These advantages arise from the fact that the Boltzmann equation is local in time. Hence, in the case of the Boltzmann equation, there is no history matrix. Consequently, one does not face any problems with computer memory and algorithms using an adaptively controlled time-step size become available. Especially the latter ones considerably speed up the numerics.

In the future it will be interesting to perform a similar comparison between the Boltzmann and the Kadanoff-Baym equations for a Yukawa-type quantum field theory including fermions. Also a treatment of the Kadanoff-Baym equations on an expanding space-time should reveal interesting results. This would finally enable one to attack the problem of leptogenesis. Independent of the comparison between the Boltzmann and the Kadanoff-Baym equations we are looking forward to learn to which extent a full non-perturbative renormalization procedure [41–46] affects the results.

Acknowledgments

TripleM would like to thank Jürgen Berges for many fruitful discussions and collaboration on related work. Furthermore we would like to thank, Mathias Garny and Patrick Huber for discussions and valuable hints. This work was supported by the "Sonderforschungsbereich

375 für Astroteilchenphysik der Deutschen Forschungsgemeinschaft”.

Appendix: Simplifying the Boltzmann Equation

The simplification of the Boltzmann equation [47] relies on the Fourier representation of the momentum conservation delta function:

$$\delta^3(\mathbf{m}) = \int \frac{d^3\xi}{(2\pi)^3} [\exp(-i\mathbf{m}\boldsymbol{\xi})] .$$

Using spherical coordinates, we find

$$\mathbf{m}\boldsymbol{\xi} = m\xi \left(\sin\vartheta_m \sin\vartheta_\xi \cos(\varphi_m - \varphi_\xi) + \cos\vartheta_m \cos\vartheta_\xi \right) .$$

Now, we consider just the integration over the solid angle. As we integrate over the whole solid angle Ω_ξ , it does not matter in which direction \mathbf{m} is pointing. The result will always be the same:

$$\int d\Omega_\xi \exp(-i\mathbf{m}\boldsymbol{\xi}) = \int d\Omega_\xi \exp(-i\mathbf{m}_0\boldsymbol{\xi}) ,$$

where we can choose $\mathbf{m}_0 = (0, 0, m)$, such that $\varphi_m = \vartheta_m = 0$. Now, we can evaluate the integral quite easily:

$$\int d\Omega_\xi \exp(-i\mathbf{m}\boldsymbol{\xi}) = \int d\Omega_\xi \exp(-im\xi \cos\vartheta_\xi) = \frac{4\pi}{m\xi} \sin(m\xi) . \quad (21)$$

After we have rewritten Eq. (15) using spherical coordinates and inserted the Fourier representation for the momentum conservation delta function, we can use Eq. (21) to perform the integrations over the solid angles. Here it is crucial first to evaluate the integrals over Ω_p , Ω_q and Ω_r , and to do the integral over Ω_ξ at last. We find:

$$\begin{aligned} \partial_t n(t, k) &= \frac{\lambda^2}{96\pi^4} \int_0^\infty dp \int_0^\infty dq \int_0^\infty dr \int_0^\infty d\xi \left[pqr \frac{\delta(E_k + E_p - E_q - E_r)}{E_k E_p E_q} \right. \\ &\quad \times \frac{1}{k\xi^2} \sin(k\xi) \sin(p\xi) \sin(q\xi) \sin(r\xi) \\ &\quad \left. \times \left((1 + n_k)(1 + n_p) n_q n_r - n_k n_p (1 + n_q)(1 + n_r) \right) \right] , \end{aligned}$$

There are only two more steps to make in order to arrive at Eq. (17). First, we define the function $D(k, p, q, r)$:

$$D(k, p, q, r) = \int_0^\infty d\xi \frac{1}{k\xi^2} \sin(k\xi) \sin(p\xi) \sin(q\xi) \sin(r\xi) .$$

This can easily be evaluated using a computer algebra program. For $k > 0$ this is

$$\begin{aligned}
D(k, p, q, r) = & \frac{\pi}{16k} \left((k - p - q - r) \text{sign}(k - p - q - r) \right. \\
& - (k + p - q - r) \text{sign}(k + p - q - r) \\
& - (k - p + q - r) \text{sign}(k - p + q - r) \\
& + (k + p + q - r) \text{sign}(k + p + q - r) \\
& - (k - p - q + r) \text{sign}(k - p - q + r) \\
& + (k + p - q + r) \text{sign}(k + p - q + r) \\
& + (k - p + q + r) \text{sign}(k - p + q + r) \\
& \left. - (k + p + q + r) \text{sign}(k + p + q + r) \right),
\end{aligned}$$

and for $k = 0$ we obtain

$$\begin{aligned}
D(0, p, q, r) = & \frac{\pi}{8} \left(\text{sign}(p + q - r) - \text{sign}(p - q - r) \right. \\
& \left. + \text{sign}(p - q + r) - \text{sign}(p + q + r) \right).
\end{aligned}$$

Second, we use the energy conservation δ function to evaluate the integral over r , using the well-known formula

$$\delta(f(r)) = \sum_{\{r_0 | f(r_0)=0\}} \frac{\delta(r - r_0)}{\left| \left(\frac{df}{dr} \right)_{r=r_0} \right|}.$$

r_0 is determined by the condition that the argument of the energy conservation δ function is zero:

$$E_k + E_p - E_q - E_{r_0} = 0. \tag{22}$$

If this condition can be satisfied, r_0 is given by

$$r_0 = r_0(t, k, p, q) = \sqrt{(E_k + E_p - E_q)^2 - M^2(t)}.$$

If k , p and q are such that condition (22) cannot be satisfied, the above square root yields a purely imaginary result and $r_0^2 < 0$. Due to the Θ function the corresponding term does not contribute to the collision integral. After these final steps we end up exactly with Eq. (17).

References

- [1] M. Fukugita and T. Yanagida, *Baryogenesis without Grand Unification*, Phys. Lett. **B174** (1986) 45

- [2] W. Buchmüller, P. Di Bari, and M. Plümacher, *Leptogenesis for pedestrians*, Ann. Phys. **315** (2005) 305
- [3] Wilfried Buchmüller and Stefan Fredenhagen, *Quantum mechanics of baryogenesis*, Phys. Lett. **B483** (2000) 217
- [4] A. D. Sakharov, *Violation of CP Invariance, C Asymmetry, and Baryon Asymmetry of the Universe*, JETP Lett. **5** (1967) 24
- [5] I. Arsene et al. (BRAHMS Collaboration), *Quark gluon plasma and color glass condensate at RHIC? The perspective from the BRAHMS experiment*, Nucl. Phys. **A757** (2005) 1
- [6] B. B. Back et al. (PHOBOS Collaboration), *The PHOBOS perspective on discoveries at RHIC*, Nucl. Phys. **A757** (2005) 28
- [7] J. Adams et al. (STAR Collaboration), *Experimental and theoretical challenges in the search for the quark gluon plasma: The STAR collaboration's critical assessment of the evidence from RHIC collisions*, Nucl. Phys. **A757** (2005) 102
- [8] K. Adcox et al. (PHENIX Collaboration), *Formation of dense partonic matter in relativistic nucleus nucleus collisions at RHIC: Experimental evaluation by the PHENIX collaboration*, Nucl. Phys. **A757** (2005) 184
- [9] Jürgen Berges, Szabolcs Borsányi, and Christof Wetterich, *Prethermalization*, Phys. Rev. Lett. **93** (2004) 142002
- [10] Gordon Baym and Leo P. Kadanoff, *Quantum Statistical Mechanics*, Benjamin, New York (1962)
- [11] P. Danielewicz, *Quantum Theory of Nonequilibrium Processes, I and II*, Ann. Phys. **152** (1984) 239 and 305
- [12] Jean-Paul Blaizot and Edmond Iancu, *The quark-gluon plasma: Collective dynamics and hard thermal loops*, Phys. Rept. **359** (2002) 355
- [13] Jürgen Berges, *Controlled nonperturbative dynamics of quantum fields out of equilibrium*, Nucl. Phys. **A699** (2002) 847
- [14] Gert Aarts and Jürgen Berges, *Nonequilibrium time evolution of the spectral function in quantum field theory*, Phys. Rev. **D64** (2001) 105010
- [15] Edward W. Kolb and Stephen Wolfram, *Baryon Number Generation in the Early Universe*, Nucl. Phys. **B172** (1980) 224
- [16] Edward W. Kolb and Michael S. Turner, *The Early Universe*, Addison-Wesley (1990)

- [17] H. S. Köhler, *Memory and correlation effects in nuclear collisions*, Phys. Rev. **C51** (1995) 3232
- [18] K. Morawetz and H. S. Köhler, *Formation of correlations and energy-conservation at short time scales*, Eur. Phys. J. **A4** (1999) 291
- [19] S. Juchem, W. Cassing, and C. Greiner, *Quantum dynamics and thermalization for out-of-equilibrium ϕ^4 theory*, Phys. Rev. **D69** (2004) 025006
- [20] Gordon Baym and Leo P. Kadanoff, *Conservation Laws and Correlation Functions*, Phys. Rev. **124** (1961) 287
- [21] Gordon Baym, *Self-Consistent Approximations in Many-Body Systems*, Phys. Rev. **127** (1962)
- [22] Yu. B. Ivanov, J. Knoll, and D. N. Voskresensky, *Self-consistent approximations to non-equilibrium many-body theory*, Nucl. Phys. **A657** (1999) 413
- [23] R. Jackiw, *Functional evaluation of the effective potential*, Phys. Rev. **D9** (1974) 1686
- [24] John M. Cornwall, R. Jackiw, and E. Tomboulis, *Effective Action for Composite Operators*, Phys. Rev. **D10** (1974) 2428
- [25] E. Calzetta and B. L. Hu, *Nonequilibrium quantum fields: Closed-time-path effective action, Wigner function and Boltzmann equation*, Phys. Rev. **D37** (1988) 2878
- [26] Yu. B. Ivanov, J. Knoll, and D. N. Voskresensky, *Resonance Transport and Kinetic Entropy*, Nucl. Phys. **A672** (2000) 313
- [27] Yu. B. Ivanov, J. Knoll, and D. N. Voskresensky, *Exact Conservation Laws of the Gradient Expanded Kadanoff-Baym Equations*, Annals Phys. **293** (2001) 126
- [28] Jürgen Berges, Szabolcs Borsányi, and Julien Serreau, *Thermalization of fermionic quantum fields*, Nucl. Phys. **B660** (2003) 51
- [29] Julian Schwinger, *Brownian Motion of a Quantum Oscillator*, J. Math. Phys. **2** (1961) 407
- [30] Pradip M. Bakshi and Kalyana T. Mahantappa, *Expectation Value Formalism in Quantum Field Theory. I and II*, J. Math. Phys. **4** (1963) 1 and 12
- [31] Leonid V. Keldysh, *Diagram Technique for Nonequilibrium Processes*, Soviet Physics JETP **20** (1965) 1018
- [32] Jürgen Berges and Markus M. Müller, *Nonequilibrium Quantum Fields with Large Fluctuations*, Progress in Nonequilibrium Green's Functions II, M. Bonitz and D. Semkat (eds.), World Scientific Publ., Singapore (2003)

- [33] S. Juchem, W. Cassing, and C. Greiner, *Nonequilibrium quantum-field dynamics and off-shell transport for ϕ^4 -theory in 2+1 dimensions*, Nucl. Phys. **A743** (2004) 92
- [34] J. Berges and Sz. Borsanyi, *Nonequilibrium quantum fields from first principles* (2005). [hep-th/0512010](#)
- [35] Jürgen Berges, Szabolcs Borsányi, and Christof Wetterich, *Isotropization far from equilibrium* (2005). [hep-ph/0505182](#)
- [36] Jürgen Berges, *Introduction to Nonequilibrium Quantum Field Theory*, AIP Conf. Proc. **739** (2005) 3
- [37] István Montvay and Gernot Münster, *Quantum fields on a lattice*, Cambridge University Press (1994)
- [38] Matteo Frigo and Steven G. Johnson, *FFTW Reference Manual*, Version 3.1 (2004)
- [39] Alejandro Arrizabalaga, Jan Smit, and Anders Tranberg, *Equilibration in ϕ^4 theory in 3+1 dimensions* (2005). [hep-ph/0503287](#)
- [40] Mark Galassi et al, *GNU Scientific Library Reference Manual*, Version 1.5 (2004). See also [48].
- [41] Hendrik van Hees and Jörn Knoll, *Renormalization in self-consistent approximation schemes at finite temperature: Theory*, Phys. Rev. **D65** (2002) 025010
- [42] Hendrik van Hees and Jörn Knoll, *Renormalization of self-consistent approximation schemes at finite temperature. II. Applications to the sunset diagram*, Phys. Rev. **D65** (2002) 105005
- [43] Hendrik van Hees and Jörn Knoll, *Renormalization in self-consistent approximation schemes at finite temperature. III. Global symmetries*, Phys. Rev. **D66** (2002) 025028
- [44] Jean-Paul Blaizot, Edmond Iancu, and Urko Reinosa, *Renormalization of phi-derivable approximations in scalar field theories*, Nucl. Phys. **A736** (2004) 149
- [45] Jürgen Berges, Szabolcs Borsányi, Urko Reinosa, and Julien Serreau, *Renormalized thermodynamics from the 2PI effective action*, Phys. Rev. **D71** (2005) 105004
- [46] Jürgen Berges, Szabolcs Borsányi, Urko Reinosa, and Julien Serreau, *Nonperturbative renormalization for 2PI effective action techniques* (2005). [hep-ph/0503240](#)
- [47] A. D. Dolgov, S. H. Hansen, and D. V. Semikoz, *Non-equilibrium corrections to the spectra of massless neutrinos in the early universe*, Nucl. Phys. **B503** (1997) 426
- [48] William H. Press et al, *Numerical Recipes in C*, Cambridge University Press (1988)